Polymer micelles for the protection and delivery of specialized pro-resolving mediators

by

Mitchell de Prinse

A thesis submitted to the Department of Chemical Engineering in conformity with the requirements for the degree of Master of Applied Science

Queen's University

Kingston, Ontario, Canada

March, 2021

Abstract

Specialized pro-resolving mediators (SPM) play a pivotal role in the resolution of acute inflammation events and have recently gained interest as a treatment for chronic inflammation. Polymer micelles are a promising approach for the delivery of these SPMs as they can protect them from oxidative degradation as well as improve their bioavailability. In this study block copolymers of poly(ethylene glycol) and poly(trimethylene carbonate-5-benzyloxy-trimethylene carbonate) (P(TMC-BTMC)) were produced via ring-opening polymerization. The BTMC units were also modified with sorbic acid in an attempt to introduce additional interactions between the micelle core and the model drug linoleic acid. The block copolymers created formed stable micelles capable of high loading of linoleic acid. *In vitro* release of linoleic acid was observed over 4 weeks and showed no signs of a burst phase. The polymer micelles also reduced the extent of oxidation of linoleic acid prior to its release compared to a linoleic acid control.

Table of Contents

List of Figures

List of Tables

Chapter 1.0 Introduction

1.1 Background

Chronic inflammatory diseases and syndromes including Crohn's disease, arthritis, allergies and asthma affect a large population of people. Currently, the treatment of these diseases involves suppressing the patient's immune system, putting them at risk of several adverse side effects including infection and stroke [1]. Recently, specialized pro-resolving mediators (SPMs) have been recognized for their role in the natural resolution of acute inflammatory events and have gained interest as a treatment for various chronic inflammatory diseases [2]. Due to their low water solubility and short half-lives *in vivo*, SPMs require a method of delivery to be an effective treatment for chronic inflammation [3][4].

Polymer micelles have been extensively studied for their ability to solubilize hydrophobic drugs in aqueous environments as well as protect them prior to release [5]. The tunable nature of polymers allow for modifications to the micelle core block, affecting micelle stability, drug loading content and drug release [6][7][8][9][10]. Currently, polysorbate 80, a generic micelle used in several commercial food and cosmetic products, is being used in a gel formulation delivering lipoxin-A4 for the treatment of eczema [11][12]. Despite positive results from this topical treatment, polysorbate 80 itself is nondegradable and has shown potentially toxic effects *in vivo*, prompting the development of new polymer micelles designed for *in vivo* delivery of SPMs [13].

The current study aimed to develop amphiphilic block polymers capable of achieving a high loading content, low critical micelle concentration (10^{-3} mM) and nanoscale size (10-200 nm) while protecting an entrapped polyunsaturated fatty acid (PUFA) used as an SPM analog from oxidative degradation. Trimethylene carbonate (TMC) and 5-benzyloxy-trimethylene carbonate (BTMC) were copolymerized via initiation with monomethoxy-poly(ethylene glycol) (PEG). For some studies, the BTMC unit was modified

through debenzylation and subsequent Steglich esterification with sorbic acid, producing a poly(5-yl sorbate trimethylene carbonate-co-trimethylene carbonate) (P(STMC-TMC)) hydrophobic block. The structures of these two polymers are displayed in Figure 1. BTMC units or STMC units were introduced to the micelle core to try and enhance the polymer-drug compatibility to allow for increased micelle stability, drug loading, and prolonged release [7][14]. The polymer micelles were formed using a simple solvent evaporation method and were loaded with linoleic acid as a model drug. Because SPMs are currently extremely expensive (~$1000/µg) a model drug was deemed appropriate for this initial study. Linoleic acid was used because it is a C18 polyunsaturated fatty acid that has very low water solubility and is prone to oxidative degradation, similar to SPMs, but is relatively inexpensive [15].

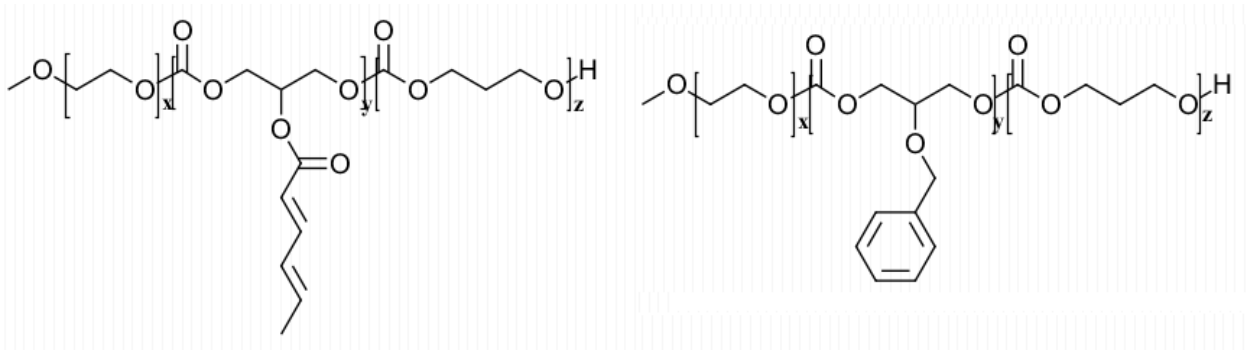

Figure 1: Chemical structures of the prepared PEG-b-P(TMC-STMC) (left) and PEG-b-P(TMC-BTMC) (right).

Chapter 2.0 Literature Review

2.1 The inflammation response

After tissue damage or injury, debris including foreign cells, particles and dead native cells are present at the wound site. Shortly after the detection of dead cells and foreign cells (pathogens), the acute inflammation response is initiated [16]. Neutrophils are then recruited to the inflammation site, are activated, and begin killing and clearing the dead cells and pathogens [17]. More leukocytes are continually recruited to the inflammation site including monocytes which develop into macrophages after entering the affected tissue, and assist in the removal of the debris [18]. These initial events of the inflammation response are orchestrated by pro-inflammatory mediators including prostaglandins, leukotrienes, cytokines and chemokines [19]. The leukocytes at the inflammation site also help produce these mediators that primarily work to upregulate the permeability of local vessels and recruit even more leukocytes [19]. This acute inflammatory response is a vital part of our immune system and its ability to fight infection. Equally as important is the resolution of this acute inflammatory response to allow for wound healing and the restoration of tissue homeostasis and function. This resolution phase is an active programmed response stimulated by anti-inflammatory and pro-resolving lipid mediators, reducing the expression of pro-inflammatory mediators and the recruitment of leukocytes to the wound [20]. Failure to resolve acute inflammation can cause enhanced prostaglandin and leukotriene production, leading to chronic inflammation and potentially fibrosis [20].

2.1.1 Specialized pro-resolving mediators

Specialized pro-resolving mediators (SPMs) are polyunsaturated fatty acids (PUFAs) enzymatically derived *in vivo* to help resolve inflammation events [19]. Several of these SPMs are produced during the acute inflammation response, making them crucial in the return to tissue homeostasis [2]. SPMs are split into four structurally distinct families of PUFAs; resolvins, protectins, lipoxins, and maresins. Each family

of SPM has specific anti-inflammatory and pro-resolving properties, but ultimately help limit the recruitment of neutrophils to the inflammation site and promote their apoptosis [21]. The apoptosis of neutrophils helps promote the phenotypic change of macrophages from pro-inflammatory (M1) to anti-inflammatory (M2) [22][23]. M2 macrophages are responsible for efferocytosis and the production of further SPMs, leading to tissue regeneration and the relief of inflammatory pain [23][24]. Efferocytosis is the process by which apoptotic cells like neutrophils are removed by macrophages, and is essential for the return to and maintenance of homeostasis [25].

2.1.2 Issues in chronic inflammation and its treatment

The pro-resolving effects of SPMs clearly have a significant impact on the resolution of acute inflammatory events [21]. However, if inflammation progresses to the chronic phase, the production of SPMs may never overcome pro-inflammatory mediators, preventing the natural transition of the immune system to resolution and tissue regeneration. These chronic conditions can be the result of an autoimmune disorder, prolonged exposure to irritants like the presence of small particles, or even untreated infections and injuries. Although some of these chronic inflammation events can be halted through the use of anti-inflammatory medication, most chronic conditions will return and persist unless medication is continually used [26]. Long term use of anti-inflammatory medication has several side effects associated with their ability to suppress the immune system, including: increased risk of peptic ulcer disease, acute renal failure, infection, and stroke [1]. As well, long term use can exacerbate pre-existing diseases like heart failure and high blood pressure [1]. Thus, SPMs have gained interest for their use as treatment for various forms of chronic inflammation, including ongoing development of resolvin-E1, maresin-1, and protectin-D1 for the treatment of neurodegenerative diseases [19]. Resolvin-E1 also has a synthetic analog currently in clinical trials for the treatment of dry eye syndrome [19]. Lipoxin-A4 has also gained interest for the treatment of eczema and asthma, reducing the severity of eczema in a

randomized controlled trial of 60 infants and decreasing LTC4-initiated bronchoprovocation in patients with asthma [12][19][27].

The main challenge associated with long term use of SPMs is that they have very short half-lives, both *in vivo* and *in vitro*, because they are susceptible to oxidation [3][4]. This susceptibility is a result of the several carbon double bonds and pendant hydroxyl units SPMs possess. Additionally, SPMs have low water solubility, which limits their bioavailability [3]. A delivery system that could help improve the bioavailability of SPMs as well as provide a barrier to oxidation prior to release would increase the efficacy of SPMs as a treatment for chronic inflammation.

2.2 Hydrophobic drug delivery

The production of new drugs is following a trend of increasing drug size and hydrophobicity [28]. This trend is problematic because the human body is a water-rich environment, causing these large hydrophobic drugs to have poor bioavailability. Several methods for improving the uptake and overall bioactivity of these large hydrophobic drugs have been employed including PEGylation and entrapment in liposomes, liquid polymers, and polymer micelles. These delivery methods also help provide a protective barrier to the drug from the external environment, benefiting drugs prone to degradation [5][29][30][31]. A delivery method of this kind could benefit the delivery of SPMs for the treatment of chronic inflammation by protecting the SPM from oxidation and improving their uptake.

2.2.1 Delivery methods

PEGylation is the method of covalent and or non-covalent bonding of poly(ethylene glycol) (PEG) chains to a molecule of interest. In pharmaceutics, PEGylation is a rapidly growing simple technique used to improve a drug's hydrophilicity. PEGylation has also been shown to extend the blood circulating life of drugs, reduce dosage frequency, and increase drug stability without diminishing drug efficacy [29].

However, PEGylated drugs can have unpredictable clearance times and may accumulate in the liver [32]. Also, the PEGylation reaction between the drug and chosen PEG end group can cause the drug to lose its bioactivity because of the reaction conditions [33]. In the case of SPMs, it could be possible to conjugate PEG to their carboxyl group without losing bioactivity via a coupling approach with 1-ethyl-3-(3-dimethylaminopropyl)carbodiimide (EDC). Although possible, PEGylation of SPMs is not the most effective method for delivery due to the localized effects of chronic inflammation and SPMs' susceptibility to oxidation. Perhaps in combination with another delivery method PEGylation could help prolong the stability of SPMs as well as their release locally.

Liposomes are membrane vesicles that have at least one lipid bilayer. The bilayers are formed by amphiphilic molecules, usually phospholipids, and are separated by aqueous compartments including an aqueous central compartment. Liposomes have been used as drug delivery vehicles for their ability to store both hydrophobic and hydrophilic drugs in their lipid bilayers and aqueous compartments, respectively. Liposomes have been found to help improve the circulation time of drugs *in vivo*, protect the drug from its environment, and also accumulate at tumors via the enhanced vascular permeability and retention effect [30][34]. However, issues with the poor stability of liposomes *in vivo* results in rapid and hard to control release rates [34]. Hydrophobic drugs with high membrane permeability, like SPMs, can also contribute to this fast release due to fast diffusion [34]. Liposomes are also prone to rapid clearance by macrophages of the reticuloendothelial system (RES), mainly from the liver and spleen [35]. The PEGylation of lipids in liposomes, as well as the addition of cholesterol, has been shown to increase liposome stability and reduce RES clearance; however these additive compounds can drastically increase the production cost and complexity of liposomes [36][37].

Injectable liquid polymers are being investigated for their use as a drug depot for proteins and hydrophobic drugs [38]. Because they can be biodegradable and are injectable, liquid polymers can

provide a minimally invasive method for sustained and local drug release. They also help to protect the loaded drugs from their aqueous environment prior to release. However, several polymers, including poly(ortho ester)s and poly(ester)s, have been shown to produce acidic degradation products, causing their own inflammation events *in vivo* and potentially damaging the loaded drugs [31][39][40]. The development of polymers that can degrade without the production of acidic by-products, like poly(5-hydroxy-trimethylene carbonate) (PHTMC) which degrades into glycerol, carbon dioxide, and low molecular weight poly(trimethylene carbonate) will help to reduce these degradation complications [41]. Overall, injectable liquid polymers are a promising approach to have a controlled and sustained release of therapeutics in a local site.

Polymeric micelles are self-assembled nanoparticle (~10-200 nm) structures formed through the aggregation of amphiphilic polymer strands above their critical micelle concentration (CMC) in solution [6]. In aqueous solution, polymeric micelles have a hydrophobic core, allowing them to harbour hydrophobic drugs as a delivery vessel. They provide protection to the entrapped drug from the aqueous environment as well as improve the drug circulation time *in vivo* [42]. Block copolymers, typically diblock or triblock, consisting of hydrophobic and hydrophilic segments are used to provide the required amphiphilic interaction. The most common hydrophilic segment used is PEG, which is used almost exclusively, causing most polymer micelle innovations to focus on the choice of hydrophobic segment [6]. In comparison to their liposome counterparts, polymer micelles are typically more stable, exhibiting CMCs in the micromolar concentration range ($>10^{-3}$ mM) [43][44]. As well, polymers can be readily modified, allowing for adaptations to the hydrophobic core and micelle surface to assist the specific application. Polymer micelles have also been used in combination with other delivery methods including hydrogels and topical formulations, thereby providing additional administration methods as well as a way to extend drug release [12][45].

One of the most common commercial polymer micelles is polysorbate 80, a polymer developed from PEGylated sorbitan and oleic acid [11]. Polysorbate 80 is used mainly as an emulsifier in foods and cosmetics, however it also finds use in pharmaceuticals [11]. This usage includes the delivery of SPMs, as polysorbate 80 loaded with lipoxin-A4 has been used in a topical cream for the treatment of eczema [12]. Although the treatment showed significant benefits as well as no adverse effects, polysorbate 80 itself is nondegradable, limiting the application to topical use [13]. Also, polysorbate 80 formulations have been associated with a number of *in vivo* adverse effects including renal and liver toxicity as well as systemic reactions like hypersensitivity [13]. These negative effects prompted an investigation into polymer micelle alternatives that are nontoxic and degradable *in vivo*, while still providing high drug loading, protection, and a sustained drug release.

2.2.2 Polymer micelle modification for drug delivery

The hydrophobic core of polymer micelles can be modified to help improve drug loading, micelle stability, drug protection, and control the rate of drug release [7][8][9][10]. Modifications can be done in several ways including: the use of copolymers as a micelle's hydrophobic block, adjusting the polymer ratio of hydrophobic to hydrophilic blocks, and through the addition or conjugation of chemical moieties to the micelle core [14][46].

The success of these adjustments largely depends on the polymer-drug compatibility; an interaction that can be very difficult to predict [14]. Several factors, including the rigidity of the drug structure as well as intermolecular forces between the polymer and drug, like hydrogen bonding, will impact the polymer-drug compatibility [47][48]. For example, dexamethasone (DEX), a type of corticosteroid used as medication for several conditions including inflammation and COVID-19, is practically insoluble in water and therefore requires a formulation to be delivered effectively [49]. Although DEX has hydrogen

bonding sites and is very hydrophobic, relatively low loading content (~0.5-2.5 wt%) was achieved in DEX-loaded micelles made from Pluronic F127 and PEG-b-poly(caprolactone) [50][51]. This low loading content may be due to the rigidity of DEX's steroid structure, hindering the interactions that would be expected to happen between DEX and the polymer, and therefore lowering their compatibility [14]. Perhaps a chemical moiety that possesses its own aromatic ring(s) could help to improve the polymer-DEX compatibility through the addition of pi-stacking covalent interactions. If this were effective, the loading of DEX could be improved and its release prolonged [10][52]. As well, the micelle stability could be improved due to the pi-bond stacking interactions caused by the aromatic rings in the micelle core [14][46][52].

The stability of polymer micelles can also be influenced through the variation of hydrophobic block chain length [6]. In general, it has been shown that as the hydrophobic block increases in size relative to the hydrophilic block, the overall micelle stability increases as indicated by a decrease in CMC [53][54]. However, as this ratio increases, there is a point at which the micelle morphology will become compromised and shift from spherical micelles to non-spherical aggregates [55]. Therefore, a balance is required between the hydrophobic and hydrophilic chain lengths such that stable and uniform micelles can be produced. Also, the degree of hydrophobicity of the core as well as the hydrophilicity of the micelle corona and their contrast can influence the micelle stability [6][46]. A study with PEG-b-poly(alkylmethacrylates) of varying degrees of hydrophobicity demonstrated that as the hydrophobicity increased, the micelle CMC decreased [56]. To further this point, zwitterionic polymer micelles have been produced that have a very strong contrast between the polarity of their hydrophilic zwitterion block and hydrophobic block. These polymer micelles display almost undetectable CMCs with reported concentrations being below 10^{-6} mM [57].

Overall, many different chemical changes can be made to polymer micelles in an attempt to improve the polymer-drug compatibility and micelle stability. However, as the complexity of polymer micelle designs increases, so does the difficulty of upscaling production and receiving approval for clinical trials [46]. This challenge is the main reason that PEG is almost exclusively used as the hydrophilic block of polymer micelles, because it is present in products that have been FDA approved [58]. Therefore, the challenge of improving polymer micelle stability and polymer-drug compatibility should also aim to be simple enough to remain feasible for larger scale production and not cause adverse effects and toxicity *in vivo.*

Chapter 3.0: Proposed approach

The delivery of hydrophobic drugs has already been explored in many studies using different methods including polymeric micelles, liquid injectable polymers, liposomes, and PEGylation. However, very few systems have been designed specifically for the delivery of SPMs. This motivates investigation into polymer micelles that are biocompatible with core blocks designed to have good compatibility with the entrapped PUFA.

Although there are currently no liquid injectable polymer systems designed for the delivery of SPMs, they seem like a promising approach for treating certain chronic inflammatory conditions that have predictable symptoms, like arthritis in a specific joint. However, because so many chronic inflammation ailments have unpredictable triggers or changing locations, like autoimmune diseases, the sustained release liquid injectable polymer systems available seem to have fewer applications for treating chronic inflammation than do polymer micelles. For that reason, polymer micelles were investigated in this study.

A micelle platform that can potentially improve upon the results of commercial micelles for the delivery of SPMs was explored in this research project. To improve the polymer-drug compatibility within the micelle core, polymers with hydrophobic blocks that provide additional intermolecular interactions for the entrapped drug were designed. This was done using the monomers trimethylene carbonate (TMC) and 5-benzyloxy-trimethylene carbonate (BTMC) to form the hydrophobic block, along with poly(ethylene glycol) (PEG) as the hydrophilic block. The BTMC repeating unit was also modified via debenzylation and subsequent Steglich esterification with sorbic acid, producing 5-yl sorbate trimethylene carbonate (STMC) repeating units. PEG was used as the hydrophilic block because of its established biocompatibility and the limited *in vivo* response it elicits [59][60]. PTMC was used as a

component of the hydrophobic block as it also has demonstrated biocompatibility *in vivo* [61][62]. Further, sorbic acid is nontoxic and metabolized by fatty acid oxidation, making it safe to use for modification of the BTMC units [63].

Chapter 4.0: Objectives

The main objective of this study was to prepare polymer micelles capable of high drug loading, oxidation protection and sustained delivery of a model SPM drug, linoleic acid.

The specific aims were as follows:

1. To synthesize PEG-b-TMC, PEG-b-P(TMC-BTMC) and PEG-b-P(TMC-STMC) copolymers.
2. To use these polymers to form micelles using a solvent evaporation technique.
3. To achieve a high linoleic acid loading, low critical micelle concentration (10^{-3} mM) and nanoscale size (10-200 nm) while maintaining a relatively narrow micelle size dispersity.
4. To study the *in vitro* release and oxidation of linoleic acid.

Chapter 5.0: Polymer Preparation and Characterization

5.1 Materials

The goal was to synthesize diblock copolymers capable of forming stable micelles in water for the loading and delivery of maresin-1. To do this, the diblock copolymer must be amphiphilic and water soluble. To provide amphiphilicity, poly(ethylene glycol) (PEG) was selected as the hydrophilic block, and poly(trimethylene carbonate) (PTMC) as the hydrophobic block.

Diblock copolymers were prepared through the ring opening polymerization of trimethylene carbonate (TMC) and 5-benzyloxy-trimethylene carbonate (BTMC) monomers with 5000 g/mol monomethoxy-PEG (PEG5000) as an initiator and either HCl-ether as catalyst or without a catalyst (Figure 2).The TMC-BTMC blocks were targeted to have the same molecular weight as the PEG5000 block with TMC-BTMC ratios of 1:0 and 3:1. The total target molecular weight ranged from 10 kDa to 12 kDa depending on the post polymerization modification of the BTMC monomer and catalyst used.

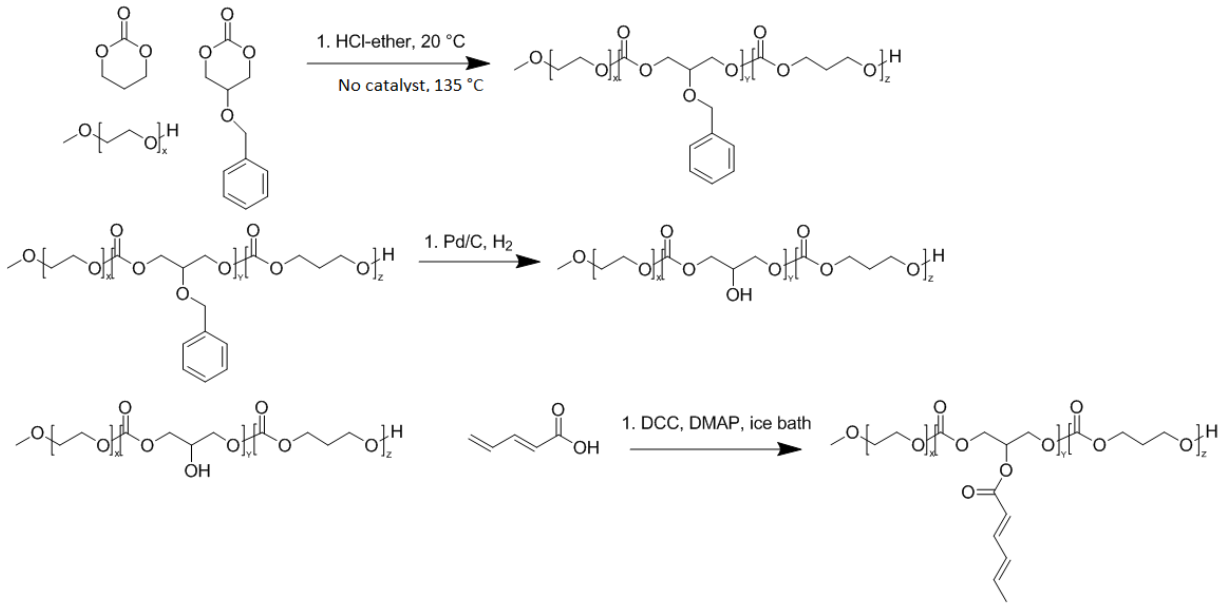

Figure 2: (From top to bottom) Ring opening polymerization reaction of trimethylene carbonate, 5-benzyloxy-trimethylene carbonate initiated by polyethylene glycol 5000 and catalyzed by HCl-ether. Debenzylation of the polymer using palladium on activated carbon as catalyst and a constant 120 psi of hydrogen. Steglich esterification of sorbic acid to the polymers pendant hydroxyl using N,N'-dicyclohexylcarbodiiimide and 4-dimethylaminopyridine as catalysts.

5.2 Synthesis and characterizations of diblock copolymers

Monomethoxy end-capped poly(ethylene glycol) (Mn 5000 Da) (PEG5000) was purchased from Acros Organics, USA. Unless otherwise described, PEG5000 was used after drying under vacuum at 40 °C for 48 h. Trimethylene carbonate (TMC) was obtained from Leapchem, Hangzhou, China. 5-benzyloxy-trimethylene carbonate (BTMC) was purchased from Obiter research LLC, USA. HCl-ether, dichloromethane (DCM), diethyl ether, methanol, and tetrahydrofuran (THF) were purchased from Fisher Scientific, Canada. Palladium on activated carbon (Pd/C), 10% Pd, unreduced was also purchased from Fisher Scientific, Canada. Sorbic acid, sorbyl chloride, 4-dimethylaminopyridine (DMAP), trimethylamine (TEA), pyridine, Celite®, d_6-dimethylsulfoxide (d_6-DMSO), and N,N'-dicyclohexylcarbodiimide (DCC) were purchased from Sigma-Aldrich, Canada.

5.2.1 Solution ring-opening polymerization

Solution polymerization of TMC and BTMC was initiated by PEG5000 in the presence of HCl-ether catalyst. A monomer to catalyst molar ratio of 5:1 was used. Dichloromethane was used as solvent and a total monomer and initiator concentration of 0.45 g/mL was used. The reaction was performed in a flame-dried round bottom flask over a stir plate, under vacuum on a Schlenk line, for 24 h at room temperature. During the addition of the reagents, the Schlenk line was switched from vacuum to nitrogen flow, preventing water and oxygen from entering the reaction. To ensure the round bottom was sealed during the reaction a thin bead of vacuum grease was spread along the fitting. After polymerization, the resulting polymer was precipitated from solution in diethyl ether three times, and excess solvent was removed under vacuum at 40 °C for at least 48 h.

5.2.2 Debenzylation of PEG-b-P(TMC-BTMC)

The polymer was debenzylated using a high pressure hydrogen reactor. The pressure of hydrogen was maintained at 120 psi for at least 24 h. The polymer was dissolved in 4:1 THF to MeOH, with a polymer concentration of approximately 0.2 g/mL. 20 wt% (with respect to polymer weight) Pd/C was used as catalyst for the reaction. The polymer solution was collected using vacuum filtration over a Celite® base and P8 Whatman filter paper. Additional THF was used to retrieve all of the polymer from the reactor and so that the Celite® filter cake had a constant flow of solvent to prevent polymer dissolution. The dilute debenzylated polymer solution was then collected in a round bottom flask and placed into a rotary evaporator to reduce the solution until it was viscous. The viscous polymer solution was then precipitated in diethyl ether three times, and excess solvent was removed under vacuum at room temperature for at least 48 h.

5.2.3 Steglich esterification of PEG-b-P(TMC-HTMC) with sorbic acid

Sorbic acid was conjugated to the pendant hydroxyl of the polymer by Steglich esterification. The polymer was first dissolved in dry DCM at a concentration of 0.2 g/mL, with 50 mol% excess sorbic acid. 10 mol% DMAP (with respect to total polymer) and 55 mol% excess DCC were used to catalyze the reaction. Sorbic acid and DMAP were added to the reaction mixture first, and then DCC was added while the vessel was in an ice bath. The reaction was left in the ice bath for at least 4 h, and the reaction ran for 24 h to ensure completion. The polymer was purified by filtering the reaction mixture with either 0.45 micron syringe tips or by vacuum filtration over three Whatman P8 filter papers, depending on the reaction scale. The remaining solution was then concentrated and precipitated in diethyl ether, twice. Excess solvent was removed under a flow of nitrogen at room temperature for at least 48 h.

5.2.4 Catalyst-free bulk polymerization

Bulk polymerization of TMC and BTMC monomer was initiated by PEG5000 in the absence of a catalyst. The reaction was performed in a flame-dried glass ampoule sealed under vacuum for 24 h in a 135 °C oven. After the initial melt of the reagents in the ampule, the reaction mixture was briefly vortexed to ensure a well-mixed system, and quickly put back in the oven. The polymer was collected by dissolution by DCM, and purified by precipitation in diethyl ether, twice. The polymer product was placed in a vacuum oven at 40 °C for 48 h to remove any excess solvent.

5.2.5 ^{1}H Nuclear magnetic resonance spectroscopy (^{1}H NMR)

Polymer number average molecular weight (M_n) and composition were determined from ^{1}H NMR spectra obtained using a 400 MHz Bruker spectrometer. The polymers were dissolved in either d_6-DMSO or $CDCl_3$ at a concentration of 45 mg/mL, and tetramethylsilane (TMS) was used as an internal reference. The solution was measured in NMR tubes at room temperature, and the data was analyzed using MestReNova lab software.

The number average molecular weight of the diblock copolymer (Mn_{total}) was determined by comparing the integration of the peak corresponding to the PEG methylene protons (I_{PEG}) to the integrations of the peaks corresponding to the methylene, methine, and methyl protons present in the TMC (I_{TMC}), BTMC (I_{BTMC}), HTMC (I_{HTMC}), and STMC (I_{STMC}) monomers. The values of I_{PEG}, I_{TMC}, I_{BTMC}, I_{HTMC}, I_{STMC}, correspond to 4, 2, 5, 1, and 3, respectively. Using this information the calculations for Mn_{total} are as follows:

$$n_{EG} = \frac{Mn_{PEG}}{Mn_{EG}} \qquad \text{Eq. 5.1}$$

$$n_{TMC} = \frac{2 * n_{EG} * I_{TMC}}{I_{PEG}} \qquad \text{Eq. 5.2}$$

$$n_{BTMC} = \frac{5 * n_{EG} * I_{BTMC}}{4 * I_{PEG}} \qquad \text{Eq. 5.3}$$

$$n_{HTMC} = \frac{n_{EG} * I_{HTMC}}{4 * I_{PEG}} \quad \text{Eq. 5.4}$$

$$n_{STMC} = \frac{3 * n_{EG} * I_{STMC}}{4 * I_{PEG}} \quad \text{Eq. 5.5}$$

Where n_{EG}, n_{TMC}, n_{BTMC}, n_{HTMC}, and n_{STMC} represent the number of repeating units of EG, TMC, BTMC, HTMC, and STMC, respectively. Using the n_i values from the equations above, the total number average molecular weight can be calculated using the monomer molecular weights:

$$Mn_{total} = Mn_{PEG} + (n_{TMC} * Mn_{TMC}) + (n_i * Mn_i) \quad \text{Eq. 5.6}$$

Where n_i and Mn_i represent the number of BTMC or STMC repeating units and molecular weight of a BTMC or STMC repeating unit, respectively, in the copolymer.

The ratio of TMC:BTMC, TMC:HTMC, and TMC:STMC, were calculated by comparing n_{TMC} to n_{BTMC}, n_{HTMC}, and n_{STMC} values. Because the target ratio for n_{TMC}:n_i was 3:1, the ratio was adjusted as if the total number of n_{TMC}:n_i units, n_T, was 4. n_T was calculated as follows:

$$n_T = n_{TMC} + n_i \quad \text{Eq. 5.7}$$

The ratio of PEG:P(nTMC) was calculated by comparing Mn_{PEG} to the sum of Mn_{TMC} and Mn_i.

5.2.6 Gel permeation chromatography (GPC)

To determine the number average molecular weight (M_n), weight average molecular weight, and the dispersity of the polymers, gel permeation chromatography (GPC) was used. The GPC used had a Waters 2690 separation module with four Styragel packed columns in series and a Waters 410 differential refractometer. High performance liquid chromatography (HPLC) grade THF was used as the mobile phase with the flowrate set at 1 mL/min. Polymer samples were prepared by dissolving 5 mg of polymer in 1 mL of HPLC grade THF, and filtering the solution through a 0.2 µm filter. Refractive index

measurements were gathered at 25 °C with distilled THF as the eluent and were calibrated to polystyrene standards.

5.3 Results and Discussion

5.3.1 Composition analysis

The success of all polymerization reactions and post-polymerization modification reactions were evaluated using ^{1}H NMR spectroscopy by calculating the molecular weight and composition of the copolymers using the peak integrals obtained from the spectra. A representative spectrum is given in Figure 3.

The molar ratio of the repeating units in the hydrophobic block (TMC:BTMC , TMC:HTMC, and TMC:STMC) were calculated from the integrations of the peaks representing the methylene groups of TMC (δ = 1.9 ppm) and either the methine units of BTMC (δ = 7.3 ppm) or the methyl unit of STMC (δ = 1.8 ppm). The hydrophilic to hydrophobic block ratio was calculated from the integrations of the methylene peaks of the PEG (δ = 3.5 ppm) and the methylene units of TMC. In most of the polymers produced, the molecular weight, comonomer ratios, and hydrophilic to hydrophobic block ratio were close to or matched the targets of 10 kDa, 3:1, and 1:1, respectively (Table 1). The HCl-ether catalyzed polymers were closer to the target molecular weight than the catalyst-free polymers, and also had lower dispersity overall.

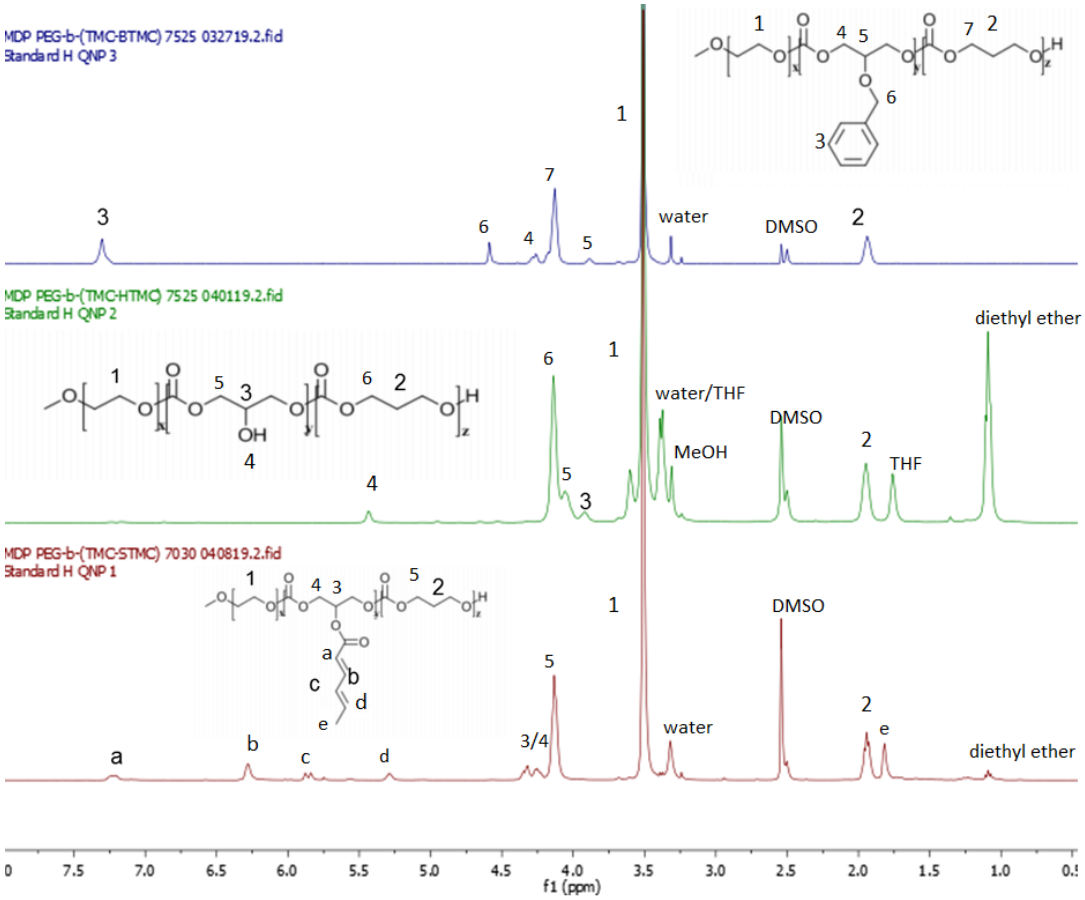

Figure 3: (From top to bottom) ^{1}H-NMR spectra of PEG-b-P(TMC-BTMC), PEG-b-P(TMC-HTMC), and PEG-b-P(TMC-STMC) in d_6-DMSO with representative peaks labelled.

Table 1: Summarized results obtained from ^{1}H-NMR and GPC analyses of the prepared polymers.

Sample Name	Catalyst	M_n (kDa) ^{1}H-NMR	M_n (kDa) GPC	M_w (kDa) GPC	Dispersity	n_{TMC}:n_i	P(nTMC): PEG
PEG-b-P(TMC-BTMC)	-	11	12.4	16.1	1.29	1.3:2.7	1.2:1.0
PEG-b-P(TMC-HTMC)	-	9	11.7	15	1.28	1.1:2.9	0.8:1.0
PEG-b-P(TMC-STMC)	-	12	10	13.5	1.36	1.2:2.8	1.4:1.0
PEG-b-P(TMC-BTMC)	HCl-ether	10	10.1	10.3	1.03	1.1:2.9	1.0:1.0
PEG-b-P(TMC-HTMC)	HCl-ether	9	8.9	9.1	1.02	0.9:3.1	0.8:1.0
PEG-b-P(TMC-STMC)	HCl-ether	10	9.8	10	1.02	1.0:3.0	1.0:1.0
PEG-b-PTMC	HCl-ether	10	10.2	10.5	1.04	1.0:0	1.0:1.0

5.4.2 Molecular weight and dispersity

All polymers catalyzed by HCl-ether at room temperature had narrow molecular weight distributions with dispersities close to 1. The obtained number average and weight average molecular weights (M_n and M_w, respectively) approached the target molecular weight of 10 kDa and those obtained from the ^{1}H-NMR spectra (Table 1).

Diblock copolymers bulk polymerized with no catalyst had broad molecular weight distributions and were bimodal, suggesting that two different polymer populations were present (Figure 4). This result is most likely due to the difference in rate of ring-opening between the TMC and BTMC monomers at the reaction conditions (130 °C, no catalyst) [64]. PEG chains that first initiated the ring-opening of TMC monomer would react faster than those that initiated BTMC monomer first, resulting in the formation of non-random copolymers. Even in the presence of 1,8-diazabicyclo[5.4.0]undec-7-ene (DBU) as catalyst, the copolymerization of TMC and BTMC was found to form block copolymers due to the difference in monomer reactivity [65].

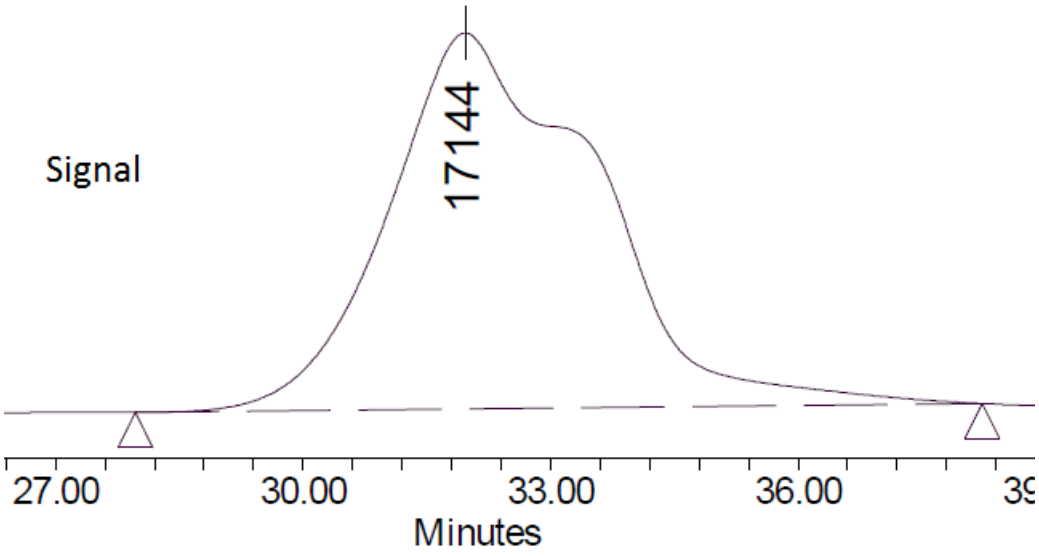

Figure 4: GPC chromatogram of the PEG-b-P(TMC-BTMC) 3:1 polymer polymerized in the presence of no catalyst, showing the formation of two separate polymer distributions as a result of non-random copolymerization.

5.4.3 Debenzylation parameters

The debenzylation efficiency of PEG-b-P(TMC-BTMC) was assessed by ^{1}H-NMR spectroscopic analysis. This was done by assessing the intensity of the peak associated with the benzyl protons at 7.3 ppm. If the reaction were fully completed, this peak should have an integral of zero. In addition, a new hydroxyl proton peak should appear at 5.4 ppm, and the methine proton peak should shift to 3.9 ppm, as shown in Figure 3. The resulting pendant hydroxyl proton peak after debenzylation was not used to determine the reaction efficiency because hydrogen bonding interactions cause the peak integral to be inconsistent, and therefore unreliable [66].

The debenzylated homopolymer, poly(5-hydroxy trimethylene carbonate) (PHTMC), is prone to degradation during some debenzylation conditions [41]. The possibility of this degradation was assessed by ^{1}H-NMR analysis after each debenzylation reaction. The degradation by-products were assigned to the peaks at 4.57 ppm and 4.3 ppm, corresponding to glycerol and partially degraded polymer chains [41]. The main influence on degradation was the concentration of polymer in solution. Polymer concentrations of 0.1 g/mL and less had larger degradation peaks in the obtained ^{1}H-NMR spectra. Polymer concentrations of 0.2 g/mL and greater had little to no degradation by-product peaks, and this concentration was used for the remainder of the debenzylation reactions performed. In addition, the higher concentration reactions went to completion faster allowing for the purification and storage of the polymer sooner. This faster reaction rate is likely the main reason that higher concentrations led to less degradation of the HTMC repeating units.

5.4.4 Esterification parameters

The efficiency of the esterification of sorbic acid to the pendant hydroxyl of the PEG-b-P(TMC-HTMC) polymer was also assessed by ^{1}H-NMR spectroscopy. The methyl protons of the conjugated sorbic acid were assigned to a chemical shift of 1.82 ppm, and the integral of this peak was compared to the

integral of the peak corresponding to the methylene protons of TMC to determine the ratio of TMC to STMC. Similar to the debenzylation of PEG-b-P(TMC-BTMC), the formation of degradation by-products was confirmed by ^{1}H-NMR analysis. This degradation was remedied by placing the reaction vessel in an ice bath prior to the addition of all reagents. The retrieved PEG-b-P(TMC-STMC) polymer also crosslinked when the unsaturated aliphatic side chains were exposed to ambient light for prolonged periods of time. This undesirable reaction was avoided by covering all glassware and containers with aluminum foil when working with the copolymer.

5.5 Conclusion

Diblock copolymers were successfully polymerized with PEG5000 as a macroinitiator and had either PTMC, P(TMC-BTMC), or P(TMC-STMC) as hydrophobic blocks. The hydrophobic block of all copolymers had TMC:BTMC or STMC monomer ratios of 1:0 and 3:1, in agreement with the targeted ratios. The polymerizations catalyzed by HCl-ether at room temperature consistently had molecular weights matching the target value and low dispersity. Polymerizations performed in the absence of catalyst at 135 °C resulted in the formation of two different polymer population distributions and as such, copolymers prepared with HCl-ether as catalyst were used in the further studies.

Chapter 6.0: Micelle Preparation, Drug Loading, and Release

6.1 Introduction

The goal was to form stable copolymer micelles in pH 7.4 phosphate-buffered saline (PBS) capable of preventing the oxidation of linoleic acid while trapping it for subsequent release. Moreover, a low critical micelle concentration and a micelle diameter between 10 to 200 µm were desired. A micelle with a lower critical micelle concentration (CMC) would indicate greater thermodynamic stability and would be less likely to aggregate [6][67]. A micelle diameter in the range of 10 to 200 nm provides a degree of targeted delivery to certain organs, potentially increasing the number of potential applications of the polymer micelles [68]. Nanoparticles smaller than 35 nm have been shown to accumulate in the kidney, while nanoparticles larger than 145 nm tend to be trapped in the spleen and or lung [69][70]. Nanoparticles between this range, 75 to 115 nm, tend to accumulate in the liver [71]. As well, the linoleic acid release profile should be prolonged and steady with minimal burst initially.

6.2 Materials

Acetonitrile, methanol, trifluoroacetic acid, linoleic acid, octanol-1, chloroform-d ($CDCl_3$), d_6-dimethylsulfoxide (d_6-DMSO) and pyrene were purchased from Sigma Aldrich, Canada. Phosphate buffered saline (PBS) salts were purchased from Fisher Scientific, Canada.

6.3 Methods

6.3.1 Micelle preparation and linoleic acid loading

Polymer micelles were prepared by first dissolving 100 mg of polymer in 1 mL of acetonitrile. 5 mL of deionized water was then added dropwise to the mixture while under continual stirring. The micellar solution was then left to stir with an open lid overnight to remove most of the acetonitrile solvent. Linoleic acid loaded micelles were prepared similarly, the only difference being that 100 mg/mL of linoleic acid was added to the acetonitrile solution. The drug-loaded micelles were then dialyzed in 2 L of deionized water for 3 h to remove excess linoleic acid not encapsulated within the copolymer micelles. The micelles were dried by lyophilisation and stored under nitrogen in a -20 °C freezer until used.

6.3.2 Dynamic light scattering (DLS)

The z-average diameter, size dispersity and CMC of the micelles were measured by dynamic light scattering (DLS) using a Zetasizer HS 3000 (Malvern Instruments, U.K.) at 25 °C. The micelle samples were dissolved in deionized water at a concentration of 0.5 mg/mL and were sonicated before measurements. Each DLS measurement was done in triplicate and the average for the three runs was calculated. The CMC was measured by DLS by serially diluting the micelle solution, and plotting the resulting count rate for each sample by its concentration. The CMC on the resulting graph is indicated by the concentration at which the slope drastically changes.

6.3.3 Pyrene assay

The CMC of the prepared micelles was also measured by pyrene assay using a Molecular Devices SpectraMax M2 UV-Vis Spectrophotometer [72]. A dilute pyrene solution in methanol was prepared by first dissolving 5 mg of pyrene in 10 mL of methanol, and then diluting this solution 20 fold with more methanol. Micelle samples were prepared by resuspending the lyophilized micelles in 200 μL PBS at 1

mg/mL, and then adding 5 μL of the dilute pyrene solution. The polymer suspension was serially diluted and the same preparation method was followed. After a short period of time to allow for the pyrene to be encapsulated, the samples were loaded into a black 96-well plate. Pyrene was excited at 334 nm and its emission was recorded at 373 nm (I_1) and 384 nm (I_3). By plotting the ratio of I_1 to I_3 at various polymer concentrations, a notable increase in the ratio should be noted as the concentration decreases. The concentration at which this point of inflection occurs was taken as the CMC for the micelles.

6.3.4 Linoleic acid release study

10 mg of linoleic acid loaded micelles were dissolved in 1 mL of PBS (measured pH=7.3). The solution was loaded into dialysis tubing with a molecular weight cut-off of 2000 g/mol. The tubing was immersed in 150-300 mL of PBS in an Erlenmeyer flask containing enough PBS such that the level in the flask reached the base of the flasks narrow neck. 4 mL of 1-octanol was then added slowly to the flask, so that it formed a layer on top of the PBS with a height between 1 and 2 inches. The dialysis setup was then placed on a stir plate in a 37 °C incubator with a stir bar and parafilm tape covering the top of the flask. At different time points 2 mL of the top 1-octanol layer was taken and 2 mL of fresh 1-octanol was added back to the dialysis setup. The linoleic acid content of the 1-octanol was measured via high performance liquid chromatography (HPLC). The same method was used for control samples, but instead free linoleic acid at a concentration of 10 mg/mL (1 mL PBS) replaced the loaded micelles in the dialysis tubing.

6.3.5 High performance liquid chromatography

The concentration of linoleic acid in the 1-octanol *in vitro* was determined by HPLC. All samples were measured in triplicate and were prepared by dissolving 100 μL of the 1-octanol release media in 900 μL of the mobile phase (a mixture of 90:10 acetonitrile/water with 0.1% trifluoroacetic acid). The HPLC

used was an Agilent 1260 Infinity, equipped with an Agilent detector and a C18 column. The flowrate was 1 mL/min, average operating pressure was 40 bar, and the injection volume was 5 µL. Linoleic acid was detected at 250 nm and had a retention time of 1.3 min. A calibration curve was obtained by dissolving linoleic acid in mobile phase at concentrations of 12.5 µg/mL to 0.781 µg/mL (Figure 5). The calibration curve was then used to determine the concentration of released linoleic acid in the 1-octanol release media. Because not all of the 1-octanol release media was replaced between each time point, the concentration after adding fresh 1-octanol back to the release setup had to be calculated using equation 6.1:

$$post\ sample\ conc._n = sample\ conc._n * \frac{total\ volume - sample\ volume}{total\ volume} \quad \text{Eq. 6.1}$$

By then comparing the previous sample's post sample concentration to the current sample's concentration, the total change in released linoleic acid over that period of time was calculated as shown in equation 6.2:

$$\Delta m = (sample\ conc._n - post\ sample\ conc._{n-1}) * total\ volume \quad \text{Eq. 6.2}$$

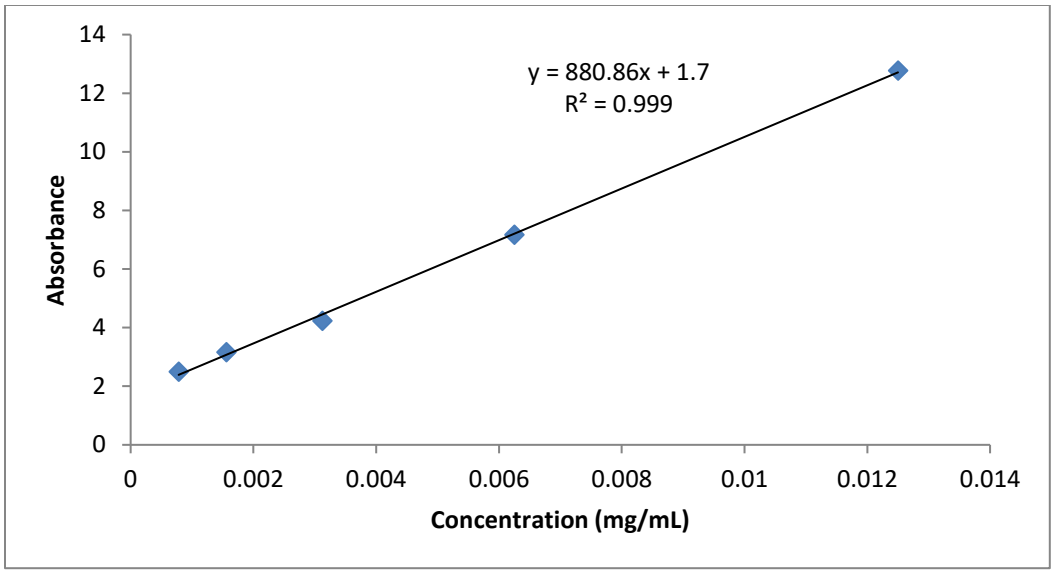

Figure 5: Calibration curve of linoleic acid obtained by HPLC.

6.3.6 ^{1}H nuclear magnetic resonance

Linoleic acid loading and shelf-life were assessed for the loaded polymer micelles by ^{1}H nuclear magnetic resonance (^{1}H NMR) using a 400 MHz Bruker spectrometer. Additionally, the polymer micelles were compared to their pre-micelle polymer spectra to ensure no chemical changes took place during the micellization process. The micelle and free linoleic acid samples were dissolved in either d_6-DMSO or $CDCl_3$ at a concentration of 45 mg/mL and 20 mg/mL, respectively. A tetramethylsilane (TMS) peak was used as the internal reference. The solution was measured in NMR tubes at room temperature, and the data was analyzed using MestReNova software.

Linoleic acid loading in the polymers was determined using ^{1}H NMR spectra integrations of poly(ethylene glycol) (PEG) methylene protons peak (I_{PEG}) compared to the integrations of linoleic acid's methyl protons peak (I_{lino}). I_{PEG} has a value of 4 protons per monomer unit and I_{lino} has a value of 3 protons per linoleic acid molecule. The number ethylene glycol units (n_{EG}) and the number of linoleic acid units (n_{lino}) per polymer was calculated as follows:

$$n_{EG} = \frac{Mn_{PEG}}{Mn_{EG}} \quad \text{Eq. 6.3}$$

$$n_{lino} = \frac{4 * n_{EG} * I_{lino}}{3 * I_{PEG}} \quad \text{Eq. 6.4}$$

Where Mn_{PEG} and Mn_{EG} are the molecular weights of the PEG initiator and ethylene glycol monomer unit, respectively. Since n_{lino} corresponds to the molar ratio of linoleic acid to polymer, the wt% of linoleic acid present in the micelles was calculated as follows:

$$m_{lino} = \frac{n_{lino} * Mn_{lino}}{Mn_{polymer}} \quad \text{Eq. 6.5}$$

$$linoleic\ acid\ wt\% = \frac{m_{lino}}{m_{lino}+1} * 100\% \quad \text{Eq. 6.6}$$

Where m_{lino} is the mass of linoleic acid per mass of polymer. Finally, the initial loading of linoleic acid within the polymer micelles was calculated by:

$$linoleic\ acid\ loading = linoleic\ acid\ wt\% * m_m \quad \text{Eq. 6.7}$$

Where m_m is the total mass of linoleic acid loaded micelles measured for use in the *in vitro* release study. The integrations of the methylene and methine groups of linoleic acid were used to confirm I_{lino}.

6.4 Results and Discussion

6.4.1 Micelle preparation

The micellization process was designed to obtain a high yield of micelles with high linoleic acid loading. The yield of micelles was greatly increased by adding water dropwise to the acetonitrile solution, as opposed to adding the acetonitrile solution dropwise to water. This result is likely due to the polymer's hydrophobicity, causing it to precipitate before forming micelles. High linoleic acid loading was achieved by adding the same concentration of linoleic acid to the acetonitrile solution as polymer (100 mg/mL). Even at this equal concentration, nearly all of the linoleic acid was encapsulated by the polymer, with linoleic acid loading close to 50 wt% even after 3 h of dialysis for all polymers tested (Table 2). This high loading content is a result of linoleic acid's hydrophobicity and results from the favourable interaction linoleic acid has with the polymer micelle cores. The loading of linoleic acid might be increased further by raising its concentration in the acetonitrile solution even more; however, due to the amount of material required this was not investigated in this study. ^{1}H-NMR spectroscopy was also used to ensure no compositional changes to the copolymer occurred during micellization. A representative spectrum for linoleic acid in PEG-b-P(TMC-STMC) micelles is given in Figure 6. The spectra of the initial polymer and micellized polymer showed no evidence of compositional changes with all peaks the same in each spectrum and corresponding to peak assignments shown in Figure 3.

Table 2: Linoleic acid loading in polymer micelles as measured by ^{1}H-NMR in $CDCl_3$.

Polymer	Linoleic acid loading (wt%)
PEG-b-PTMC	46 +/- 5
PEG-b-P(TMC-BTMC)	50 +/- 5
PEG-b-P(TMC-STMC)	45 +/- 5

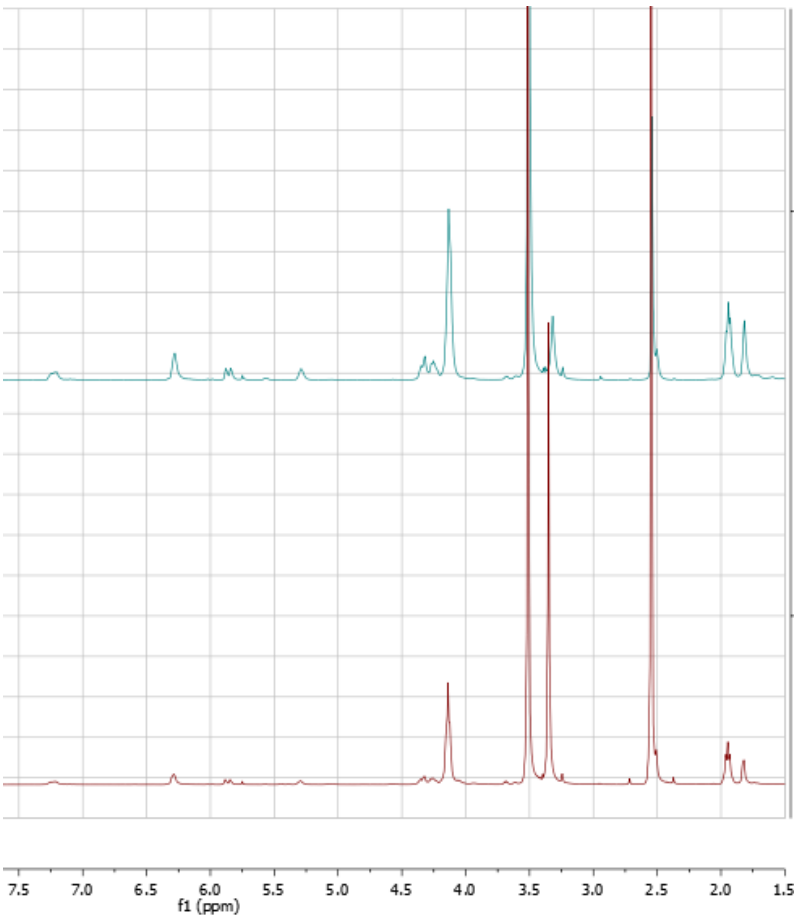

Figure 6: The ^{1}H-NMR spectra of PEG-b-P(TMC-STMC) before (top) and after micellization (bottom) were obtained in d_6-DMSO.

6.4.2 Micelle average diameter and dispersity

The goal was to obtain micelles with a size dispersity of 0.2 or less and a diameter in the range of 20-200 nm. These parameters are deemed suitable for nanoparticles being used *in vivo* in biomedical applications [70][73]. The solvent evaporation method successfully produced polymer micelles close to 100 nm in size and with a size dispersity less than 0.2 for all polymers used (Table 3). However, the linoleic acid loaded micelles were larger and more disperse, approaching diameters close to 200 nm and dispersity greater than 0.2. This is expected behaviour and is displayed extensively in the literature [73].

Although the linoleic acid loaded micelles surpassed the dispersity goal and almost the size, the size and dispersity can be reduced by decreasing: the overall polymer molecular weight, the ratio of hydrophobic block to hydrophilic block, and the amount of linoleic acid loading [6][74]. Depending on the intended application, these parameters may be tuned to achieve the desired size and dispersity of polymer micelle.

Table 3: Z-Avg diameter and size dispersity of the polymer micelles with and without linoleic acid.

Sample Name	Z-Avg d (nm)	Size Dispersity
PEG-b-P(TMC-STMC) w/ linoleic acid	176 +/- 2	0.254 +/- 0.003
PEG-b-P(TMC-BTMC) w/ linoleic acid	159 +/- 2	0.249 +/- 0.009
PEG-b-PTMC w/ linoleic acid	176 +/- 1	0.26 +/- 0.01
PEG-b-P(TMC-STMC)	125 +/- 1	0.17 +/- 0.01
PEG-b-P(TMC-BTMC)	113 +/- 1	0.194 +/- 0.004
PEG-b-PTMC	123 +/- 1	0.18 +/- 0.01

6.4.3 Critical micelle concentration (CMC)

The CMC was estimated for the linoleic acid loaded polymer micelles using a pyrene assay and by DLS. The CMC is indicated using the pyrene assay by the concentration at the point of inflection that occurs as the solution is diluted (Figure 7). The CMC was also measured by DLS, by finding the concentration that the slope drastically changes (Figure 8). In general the polymers exhibited a CMC from both the DLS and pyrene assay data of or below 0.001 mM in PBS and deionized water, which is typical of stable polymer micelles in water (Table 4) [43][44].

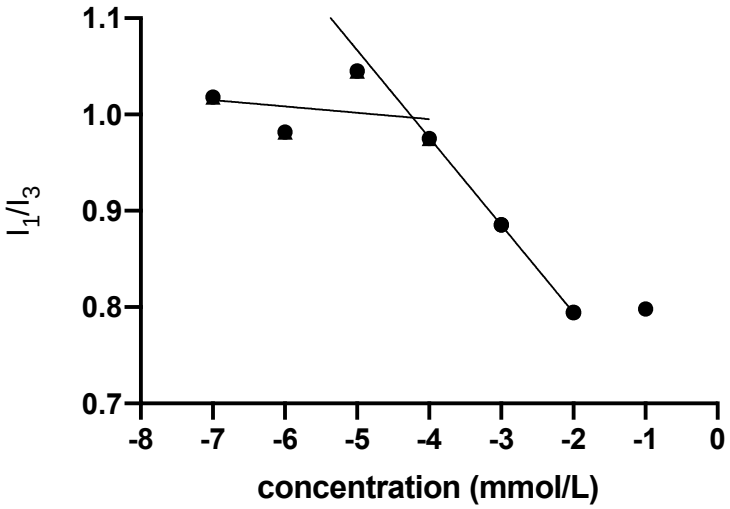

Figure 7: Pyrene assay results obtained for PEG-b-P(TMC-BTMC) from an UV-vis spectrophotometer signifying that the linoleic acid loaded polymer has a CMC close to 0.001 mM in PBS.

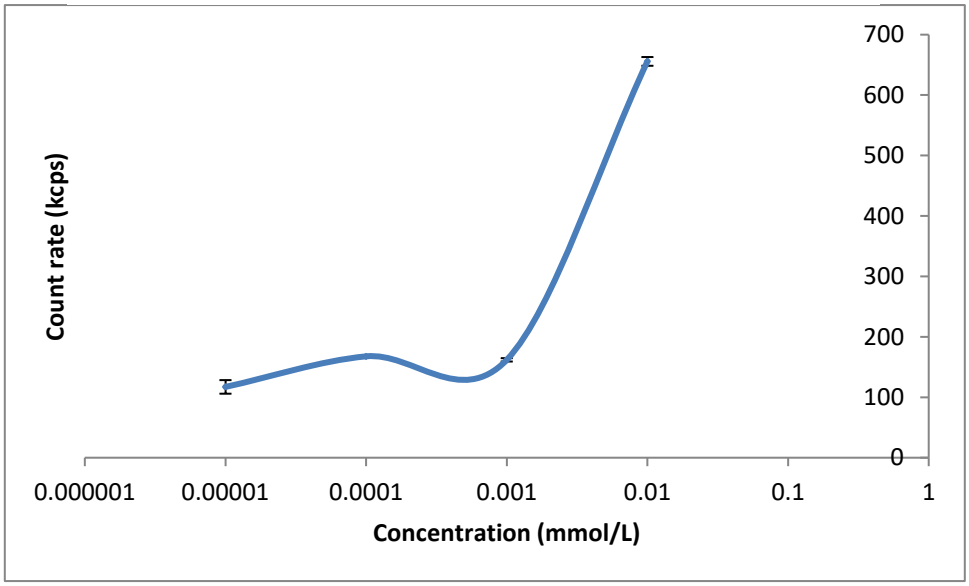

Figure 8: DLS data for PEG-b-P(TMC-STMC) micelles, showing that the CMC is less than 0.001 mM in deionized water.

Table 4: CMC data obtained from DLS and a pyrene assay for the polymer micelles.

Polymer	Pyrene Assay CMC Data (mM)	DLS CMC Data (mM)
PEG-b-P(TMC-BTMC)	1.3E-03	1.0E-04
PEG-b-P(TMC-STMC)	7.3E-04	1.0E-03
PEG-b-PTMC	2.0E-03	1.0E-03

6.4.4 Shelf life

The shelf life over 3 months of the linoleic acid loaded micelles was assessed by ^{1}H-NMR spectroscopy by storing the lyophilized micelles at room temperature in a sealed vial under a nitrogen atmosphere. No compositional change or signs of linoleic acid oxidation were noted over the three months of storage (Figure 9).

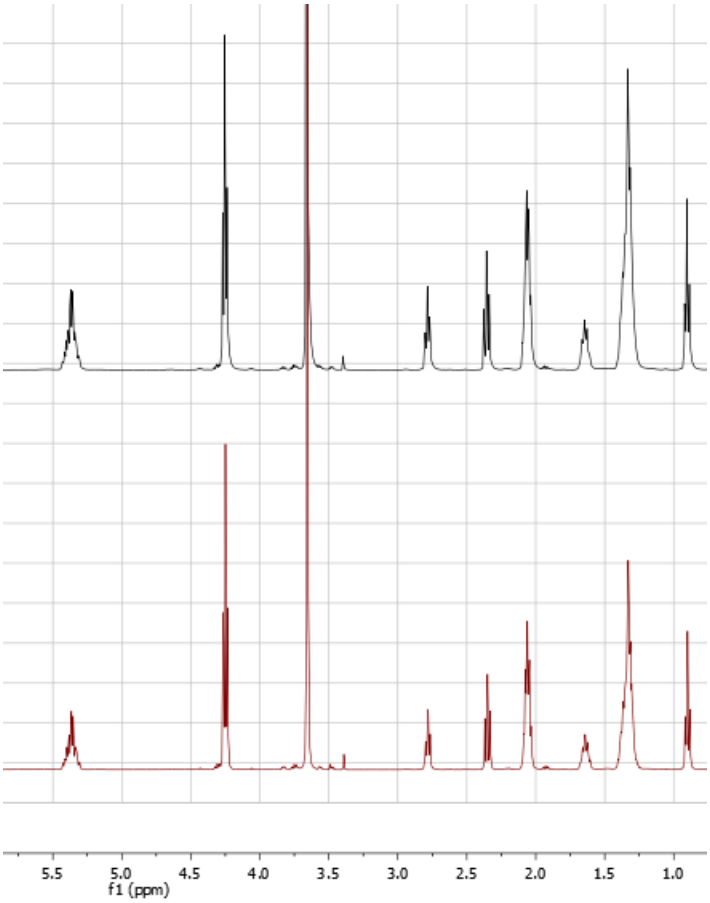

Figure 9: ^{1}H-NMR spectra of linoleic acid loaded PEG-b-PTMC micelles after lyophilisation (top) and after 3 months of storage at room temperature under nitrogen (bottom) in $CDCl_3$.

6.4.5 *In vitro* linoleic acid release

Linoleic acid release from polymer micelles *in vitro* was followed over 4 weeks (Figure 10). No signs of a burst release were observed, signifying that the short dialysis period did remove residual free linoleic acid. All three release profiles shared a similar linear release rate over the first 7-10 days, with PEG-b-PTMC micelles having a slightly faster release. This slightly faster release could be due to reduced linoleic acid affinity for the PTMC block when compared to P(TMC-BTMC) and P(TMC-STMC) core blocks. However, this effect only has a slight impact on the total release, and all three profiles reached a plateau after only 9-20% total linoleic acid mass had been released. Having a plateau at such a small percent total release can signify several things including: the released or encapsulated linoleic acid was oxidized into stearic acid and/or the linoleic acid has overwhelming affinity for the micelle core as well as underwhelming water solubility causing it to resist further release.

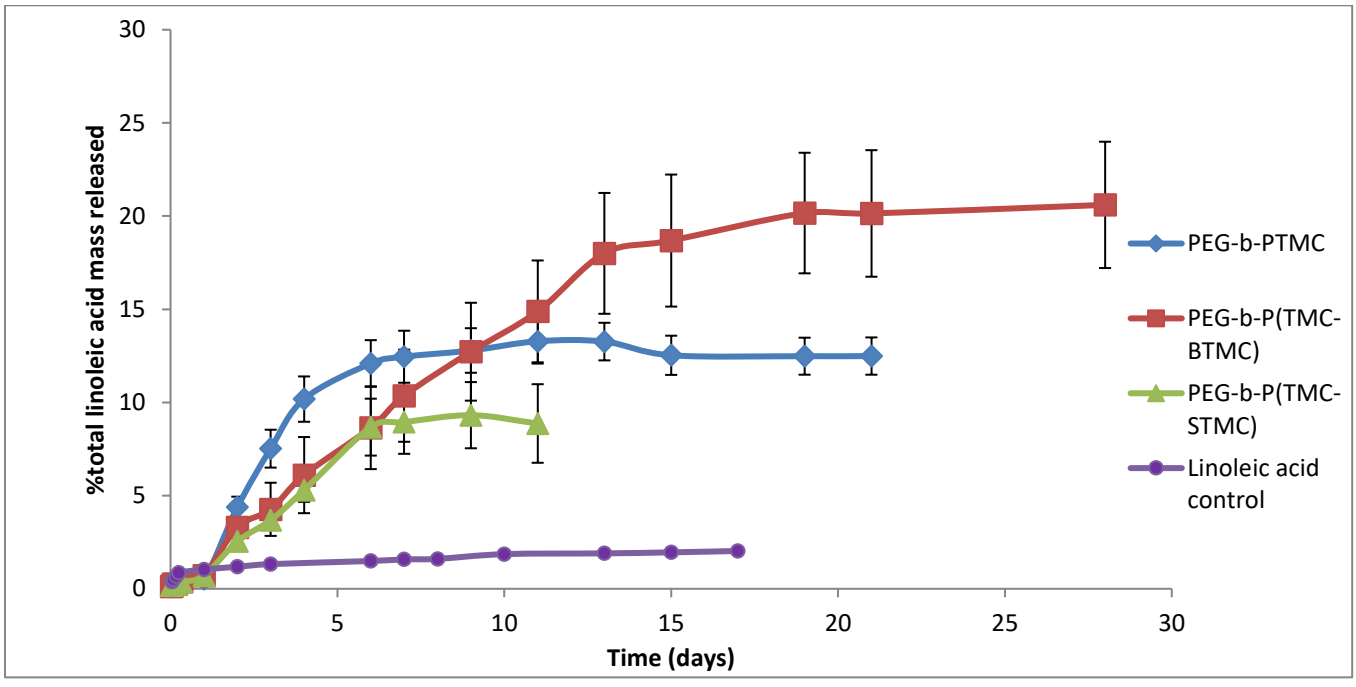

Figure 10: *In vitro* linoleic acid mass release over time as determined by HPLC and ^{1}H-NMR.

Unlike linoleic acid that possesses double bonds giving it some light absorbance, stearic acid contains no fluorophores making it practically undetectable by HPLC. Additionally, the concentration of the released linoleic acid and subsequently stearic acid is very low, making it also almost undetectable by ^{1}H-NMR. The remaining micelle solution for each polymer was retrieved from the dialysis bags after the *in vitro* release had reached a plateau for a few time points, and was lyophilized over 48 h. The lyophilized remaining loaded micelle was then dissolved in $CDCl_3$ and examined using ^{1}H-NMR spectroscopy. From all of the spectra several stearic acid-linoleic acid shared peaks (2.36, 1.65, 1.34, and 0.91 ppm) were evident; however, linoleic acid specific peaks (5.37 and 2.79 ppm) were barely noticeable (Figure 11). This finding indicates that most of the remaining linoleic acid within the micelles had oxidized and that there was a noticeable amount of stearic acid encapsulated in all of the polymer micelles after the 3-4 weeks release in PBS. The remaining solution from the linoleic acid control did not yield a ^{1}H-NMR spectrum with visible peaks, probably because the dialysis tubing used had a MWCO of 2000 g/mol. Based on Figure 11, it is likely that the majority of the linoleic acid control had oxidized, and therefore was undetectable by HPLC leading to its minimal release. Based on this analysis, it can be concluded that the polymer micelles reduced the oxidation of linoleic acid compared to the linoleic acid control.

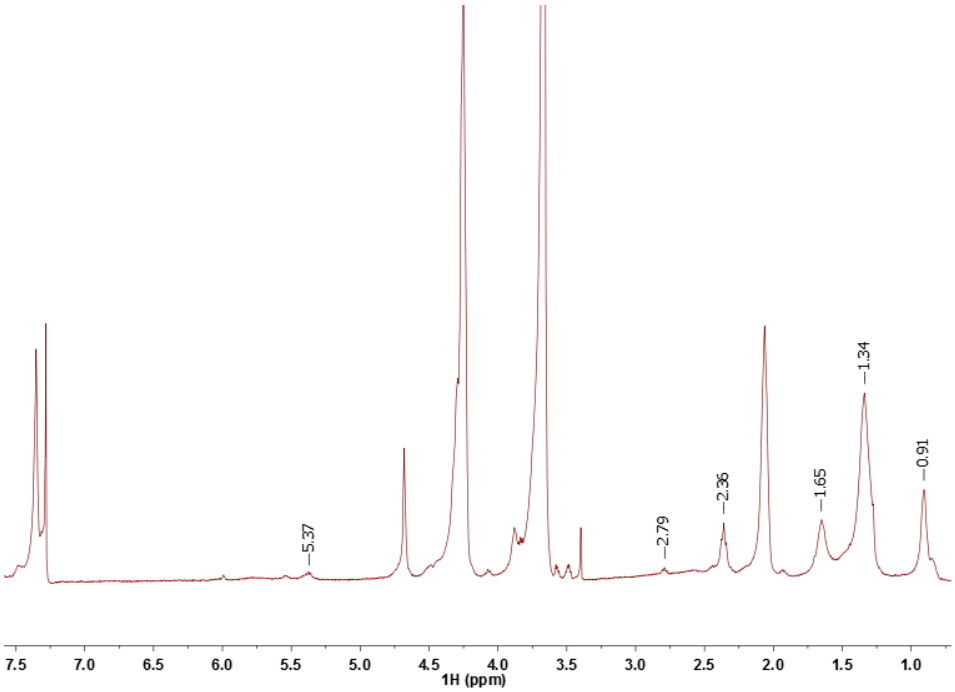

Figure 11: ^{1}H-NMR of the remaining linoleic acid loaded PEG-b-P(TMC-BTMC) (run #2) micelles after 4 weeks of release in PBS using $CDCl_3$. Peaks at 0.91, 1.34, 1.65, and 2.36 ppm signify stearic acid-linoleic acid shared peaks while peaks at 2.79 and 5.37 ppm signify linoleic acid specific peaks.

The remaining stearic acid present in the micelles was estimated by comparing the stearic acid methyl peaks (0.91 ppm) to the methylene proton peaks of PEG (3.7 ppm) and assuming all of the remaining linoleic acid had oxidized to stearic acid. Using these values as well as the final amount of released linoleic acid as measured by HPLC, the amount of released stearic acid was estimated. These results are summarized in Table 5. Overall, the majority of the linoleic acid was oxidized to stearic acid for all micelles, but the PEG-b-P(TMC-BTMC) micelles seemed to protect the linoleic acid from oxidation the best. As well, both PEG-b-P(TMC-BTMC) and PEG-b-P(TMC-STMC) micelles outperformed the PEG-b-PTMC micelles at protecting the linoleic acid from oxidation.

Table 5: Summary of mass balance results based on the measured linoleic acid released and the remaining stearic acid entrapped in the micelles post-release.

Polymer	% of initial linoleic remaining (as stearic acid)	% linoleic acid released	Approximate % linoleic acid released as stearic acid
PEG-b-PTMC	30 +/- 4	13 +/- 1	55%
PEG-b-P(TMC-BTMC)	38 +/- 4	20 +/- 3	40%
PEG-b-P(TMC-STMC)	50 +/- 10	9 +/- 2	40%

6.5 Conclusion

The copolymers investigated were able to form stable micelles in PBS with relatively low dispersity and sizes in the range of 100-200 nm, even after the loading of 50 wt% linoleic acid. The polymer showed no compositional changes after forming micelles, and the loaded PEG-b-PTMC micelles showed no linoleic acid oxidation or compositional changes after 3 months of storage at room temperature under nitrogen. The *in vitro* release profile of linoleic acid in PBS was similar between the polymers tested and showed no signs of a burst release, plateauing after 2-3 weeks of release. Only 9%-20% of the total initial linoleic acid mass released from the polymer micelles over this time period, with the majority of the linoleic acid remaining within the micelles oxidizing to stearic acid. When compared to the linoleic acid control the

polymer micelles reduced the oxidation of linoleic acid in PBS, with PEG-b-P(TMC-BTMC) loaded micelles performing the best overall.

Chapter 7.0: Summary and Conclusions

Diblock copolymers PEG-b-PTMC, PEG-b-P(TMC-BTMC) and PEG-b-P(TMC-STMC) were successfully produced and characterized. Polymers catalyzed by HCl-ether provided molecular weights close to the target and had narrow molar mass dispersity. These polymers were then micellized and loaded with 50 wt% linoleic acid as a model SPM, and resulted in the formation of stable micelles with CMCs in the range of 0.001 mM, z-avg diameters between 100-200 nm, and size dispersity close to 0.2.

The loaded polymer micelles showed no compositional changes after micellization and the PEG-b-PTMC micelles showed no compositional changes after 3 months of storage at room temperature. Similar linoleic acid release profiles were observed *in vitro* over 4 weeks for the polymers tested, with linoleic acid release reaching a plateau after the first 2-3 weeks of release with no burst release. The majority of the encapsulated and released linoleic acid oxidized to stearic acid, with only 9%-20% total linoleic acid release after 4 weeks. Despite this degree of oxidation, when compared to the micelle-free control the polymer micelles significantly reduced the extent of oxidation of linoleic acid. PEG-b-P(TMC-BTMC) and PEG-b-P(TMC-STMC) micelles protected linoleic acid from oxidation better than PEG-b-PTMC micelles did, with PEG-b-P(TMC-BTMC) micelles performing the best overall.

Overall, the polymer micelles produced were capable of prolonging the release and stability of the loaded linoleic acid. The micelles were stable and able to achieve high loading, making them an attractive approach for the protection and delivery of SPMs.

Chapter 8.0: Recommendations

The results of this study warrant further work with the polymer micelles involving the encapsulation of a more relevant molecule such as docosahexaenoic acid or an SPM. As well, better oxidation data could be obtained for the *in vitro* release study by measuring the micelles by ^{1}H-NMR at earlier time points. This could help provide information on how fast the linoleic acid is oxidizing within the micelles. Including a commercial micelle in the *in vitro* release study as an additional control could also be a useful study for comparison.

Bibliography

1. Marcum, Z. A. & Hanlon J. T. Recognizing the risks of chronic nonsteroidal anti-inflammatory drug use in older adults. *Ann. Longterm Care.* **18,** 24-27 (2010).

2. Serhan, C. N. Pro-resolving lipid mediators are leads for resolution physiology. *Nature* **510,** 92-101 (2014).

3. Gorji, M. *et al*. Polymeric pharmaceutical nanoparticles developed by electrospray, in *Nanostructures for Novel Therapy,* 1st ed. Elsevier, 2017, pp. 137-164.

4. Mozurkewich, E. L. *et al*. Pathway markers for pro-resolving lipid mediators in maternal and umbilical cord blood: a secondary analysis of the mothers, omega-3, and mental health study. *Front. Pharmacol* (2016).

5. Debe, M. S. *et al*. Polymer-based nanomaterials for drug-delivery carriers, in *Nanocarriers for Drug Delivery,* 1st ed. Elsevier, 2019, pp. 531-556.

6. Shoichet, M. S. *et al*. Polymeric micelle stability. *Nano Today* **7,** 53-65 (2012).

7. Lee, J. Y. *et al*. Incorporation and release behavior of hydrophobic drug in functionalized poly(D,L-lactide)-block-poly(ethylene oxide) micelles. *J. Control. Release* **94,** 323—335 (2004).

8. Lin, L. *et al.* Tuning core versus shell dimensions to adjust the performance of nanoscopic containers for the loading and release of doxorubicin. *J. Controlled Release* **152,** 37-48 (2011).

9. Ebrahim Attia, A. B. *et al.* Mixed micelles self-assembled from block copolymers for drug delivery. *Curr. Opin. Colloid Interface Sci.* **16,** 182-194 (2011).

10. Bariana, M. *et al.* Tuning drug loading and release properties of diatom silica microparticles by surface modifications. *Int. J. Pharm.* **443,** 230-241 (2013).

11. Kinyanjui, T. *et al*. Organic emulsifiers, in *Encyclopedia of Food Sciences and Nutrition,* 2nd ed. Elsevier, 2003, pp. 2070-2077.

12. Wu, S. H. *et al*. Efficacy and safety of 15(R/S)-methyl-lipoxin A4 in topical treatment of infantile eczema. *Paediatric Dermatology* **168,** 172-178 (2013).

13. Schwartzberg, L. S. & Navari, R. M. Safety of polysorbate 80 in the oncology setting. *Advances in Therapy* **35,** 754-767 (2018).

14. Luxenhofer, R. *et al.* Like dissolves like? A comprehensive evaluation of partial solubility parameters to predict polymer-drug compatibility in ultrahigh drug-loaded polymer micelles. *Biomacromolecules* **20,** 3041-3056 (2019).

15. Mabrouk, A. F. & Dugan Jr., L. R. Solubility of linoleic acid in aqueous solutions and its reaction with water. *Journal of the American Oil Chemists Society* **38,** 9-13 (1961).

16. Nathan, C. Points of control in inflammation. *Nature* **420**, 846–852 (2002).

17. Vaporciyan, A. A. *et al*. Involvement of platelet-endothelial cell adhesion molecule-1 in neutrophil recruitment *in vivo*. *Science* **262**, 1580–1582 (1993).

18. Geissman, F. *et al.* Development of monocytes, macrophages and dendritic cells. *Science* **327,** 656-661 (2010).

19. Levy, B. D. & Basil, M. C. Specialized pro-resolving mediators: endogenous regulators of infection and inflammation. *Nature Reviews Immunology* **16,** 51-67 (2016).

20. Serhan, C. N. *et al.* The resolution code of acute inflammation: Novel pro-resolving lipid mediators in resolution. *Seminars in Immunology* **27,** 200-215 (2015).

21. Buckley, C. D., Gilroy, D. W. & Serhan, C. N. Proresolving lipid mediators and mechanisms in the resolution of acute inflammation. *Immunity* **40**, 315–327 (2014).

22. Savill, J. Apoptosis. Phagocytic docking without shocking. *Nature* **392**, 442–443 (1998)

23. Dalli, J. & Serhan, C. N. Specific lipid mediator signatures of human phagocytes: microparticles stimulate macrophage efferocytosis and pro-resolving mediators. *Blood* **120**, 60–72 (2012).

24. Freire-de-Lima, C. G. et al. Apoptotic cells, through transforming growth factor-β, coordinately induce anti-inflammatory and suppress pro-inflammatory eicosanoid and NO synthesis in murine macrophages. *J. Biol. Chem.* **281**, 38376–38384 (2006).

25. Tabas, I. et al. Efferocytosis in health and disease. *Nature Reviews Immunology* **20,** 254-267 (2020).

26. Crohn's and Colitis Foundation of Canada, "the impact of inflammatory bowel disease in canada 2012 final report and recommendations," Toronto, 2012.

27. Hisada, T. *et al.* Are specialized pro-resolving mediators promising therapeutics agents for severe bronchial asthma? *J. Thorac. Dis.* **9,** 4266-4269 (2017).

28. Lipinsky, C. A. Drug-like properties and the causes of poor solubility and poor permeability. *J. Pharmacol Toxicol Methods* **44,** 235-249 (2000).

29. Milla, P. *et al.* PEGylation of proteins and liposomes: a powerful and flexible strategy to improve the drug delivery. *Curr. Drug Metab.* **13,** 105-119 (2012).

30. Hua, S. *et al.* Advances and challenges of liposome assisted drug delivery. *Front. Pharmacol.* (2015).

31. Amsden, B. G. Liquid, injectable, hydrophobic and biodegradable polymers as drug delivery vehicles. *Macromolecular Bioscience* **10,** 825-835 (2010).

32. Kawai, F. Microbial degradation of polyethers. *Applied Microbiology and Biotechnology* **58,** 30-38 (2002).

33. Pasut, G. & Veronese, F. M. State of the art in PEGylation: The great versatility achieved after forty years of research. *Journal of Controlled Release* **161,** 461-472 (2012).

34. Hua, S. & Wu, S. Y. The use of lipid-based nanocarriers for targeted pain therapies. *Front. Pharmacol* (2013).

35. Forssen, E. & Willis, M. Ligand-targeted liposomes. *Advanced Drug Delivery Reviews* **29,** 249-271 (1998).

36. Laverman, P. *et al.* Liposomes for scintigraphic detection of infection and inflammation. *Advanced Drug Delivery Reviews* **37,** 225-235 (1999).

37. Maruyama, K. PEG-Immunoliposome. *Bioscience Rep.* **22,** 251-266 (2002).

38. Amsden, B. & Hatefi, A. Biodegradable injectable in situ forming drug delivery systems. *Journal of Controlled Release* **80,** 9-28 (2002).

39. van de Weert, M. *et al.* Semisolid, self-catalyzed poly(ortho ester)s as controlled-release systems: protein release and protein stability issues. *Journal of Pharmaceutical Sciences* **91,** 1065-1074 (2002).

40. Ekholm, M. *et al.* Histological study of tissue reactions to Ɛ-caprolactone-lactide copolymer in paste form. *Biomaterials* **20,** 1257-1262 (1999).

41. Amsden, B. G. *et al.* Degradation of poly(5-hydroxy-trimethylene carbonate) in aqueous environments. *Polymer Degradation and Stability* **158,** 83-91 (2018).

42. Kraatz, H-B. *et al.* Polymeric micelles as drug delivery vehicles. *RSC Advances* **4,** 17028-17038 (2014).

43. Maysinger, D. *et al.* Fate of micelles and quantum dots in cells. *Eur J Pharm Biopharm.* **65,** 270-281 (2007).

44. Diezi, T. A. *et al.* Enhance stability of PEG-block-poly(N-hexyl stearate L-aspartamide) micelles in the presence of serum proteins. *Mol Pharm.* **7,** 1355-1360 (2010).

45. Hedrick, J. L. *et al.* Biodegradable strain-promoted click hydrogels for encapsulation of drug-loaded nanoparticles and sustained release of therapeutics. *Biomacromolecules* **18,** 2277-2285 (2017).

46. Cao, Z. *et al.* Strategies to improve micelle stability for drug delivery. *Nano Research* **11,** 4985-4998 (2018).

47. Rhee, S. G. H2O2, a necessary evil for cell signaling. *Science* **312,** 1882–1883 (2006).

48. Lv, S. *et al.* High drug loading and sub-quantitative loading efficiency of polymeric micelles driven by donor-receptor coordination interactions. *J. Am. Chem. Soc.* **140,** 1235-1238 (2018).

49. de Gans, J. *et al.* Dexamethasone in adults with bacterial meningitis. *N. Engl. J. Med.* **347,** 1549-1556 (2002).

50. Pepic, I. *et al.* A nonionic surfactant/chitosan micelle system in an innovative eye drop formulation. *J. Pharm. Sci.* **99,** 4317-4325 (2010).

51. Wang, Q. *et al.* Targeted delivery of low-dose dexamethasone using PCL-PEG micelles for effective treatment of rheumatoid arthritis. *J. Controllled Release* **230,** 64-72 (2016).

52. Wishart, D. S. *et al.* Application of solid phase peptide synthesis to engineering PEO-peptide block copolymers for drug delivery. *Colloids and Surfaces B: Biointerfaces* **30,** 323-334 (2003).

53. Gaucher, G. *et al.* Block copolymer micelles: preparation, characterization and application in drug delivery. *J. Control. Release* **109,** 169-188 (2005).

54. Kwon, G. S. e*t al.* The effects of acyl chain length on the micelle properties of poly(ethylene oxide)-block-poly(N-hexyl-L-aspartamide)-acyl conjugates. *J Biomater. Sci Polym. Ed.* **13,** 991-1006 (2002).

55. Gadt, T. *et al.* Complex and hierarchical micelle architectures from diblock copolymers using living, crystallization-driven polymerizations. *Nat Mater.* **8,** 144-150 (2009).

56. Ranger, M. *et al.* From well-defined diblock copolymers prepared by a versatile atom transfer radical polymerization method to supramolecular assemblies. *J. Polym. Sci. A: Polym. Chem.* **39,** 3861-3874 (2001).

57. Lu, Y. *et al.* Micelles with ultralow critical micelle concentration as carriers for drug delivery. *Nat. Biomed. Eng.* **1,** 318–325 (2018).

58. Cash, B. D. & Lacy, B. E. Systematic review: fda-approved prescription medications for adults with constipation. *Gastroenterol Hepatol* **2,** 736-749 (2006).

59. Alconcel, S. N. S., Baas, A. S. & Maynard, H. D. FDA-approved poly(ethylene glycol)–protein conjugate drugs. *Polymer Chemistry* **2,** 1442 (2011).

60. Zhu, J. Bioactive modification of poly(ethylene glycol) hydrogels for tissue engineering. *Biomaterials* **31,** 4639–4656 (2010).

61. Zhu, K. J. *et al.* Surface biodegradable copolymers-poly(D,L-lactide-co-1-methyl-1,3-trimethylene carbonate) and poly(D,L-lactide-co-2,2-dimethyl-1,3-trimethylene carbonate): preparation, characterization and biodegradation characteristics *in vivo. Polymer* **39,** 4409-4415 (1998).

62. Pitt, C. G. *et al.* Synthesis, properties, and biodegradation of poly(1,3-trimethylene carbonate). *Macromolecules* **24,** 1736-1740 (1991).

63. Reddy, S. M. & Surekha, M. Preservatives | classification and properties. *Encylocpedia of Food Microbiology* **2,** 69-75 (2014).

64. Amsden, B. G. *et al.* Dithiol-PEG-PDLLA micelles: preparation and evaluation as potential topical ocular delivery vehicle. *Biomacromolecules* **15,** 1346-1354 (2014).

65. Amsden, B. G. *et al*. Liquid degradable poly(trimethylen-carbonate-co-5-hydroxy-trimethylene carbonate): an injectable drug delivery vehicle for acid-sensitive Drugs. *Mol. Pharmaceutics* **17,** 1363-1376 (2020).

66. Hedrick, J. L. *et al.* Guanidine and amidine organocatalysts for ring-opening polymerizations of cyclic esters. *Macromolecules* **39,** 8574-8583 (2006).

67. Gerothanassis, I. P. *et al.* 1H-NMR as a structural and analytical tool of intra- and intermolecular hydrogen bonds of phenol-containing natural products and model Compounds. *Molecules* **19,** 13643-13682 (2014).

68. Doroodchi, E. *et al.* Influence of primary particle size distribution on nanoparticles aggregation and suspension yield stress: A theoretical study. *Powder Technology* **223,** 3-11 (2012).

69. Jain, A. K. & Thareja, S. In vitro and in vivo characterization of pharmaceutical nanocarriers used for drug delivery. *Artificial Cells, Nanomedicine, and Biotech.* **47,** 524-539 (2019).

70. Jing, X. *et al.* Size-dependent biodistribution and antitumor efficacy of polymer micelle drug delivery systems. *Journal of Mat. Chem. B* **34** (2013).

71. Ferrari, M. *et al.* Principles of nanoparticle design for overcoming biological barriers to drug delivery. *Nature biotech.* **33,** 941-951 (2015).

72. Montenegro, L. *et al.* Determination of critical micelle concentration of some surfactants by three technique. *J. Chem. Educ.* **74,** 1227 (1997).

73. Clarke, S. Development of hierarchical magnetic nanocomposite materials for biomedical applications. Ph.D. Thesis, Dublin City University, Northside, Dublin, (2013).

74. Stenzel, M. H. *et al.* The effect of drug loading on micelle properties: solid-state nmr as a tool to gain structural insight. *Drug Delivery* **56,** 8441-8445 (2017).

Appendix

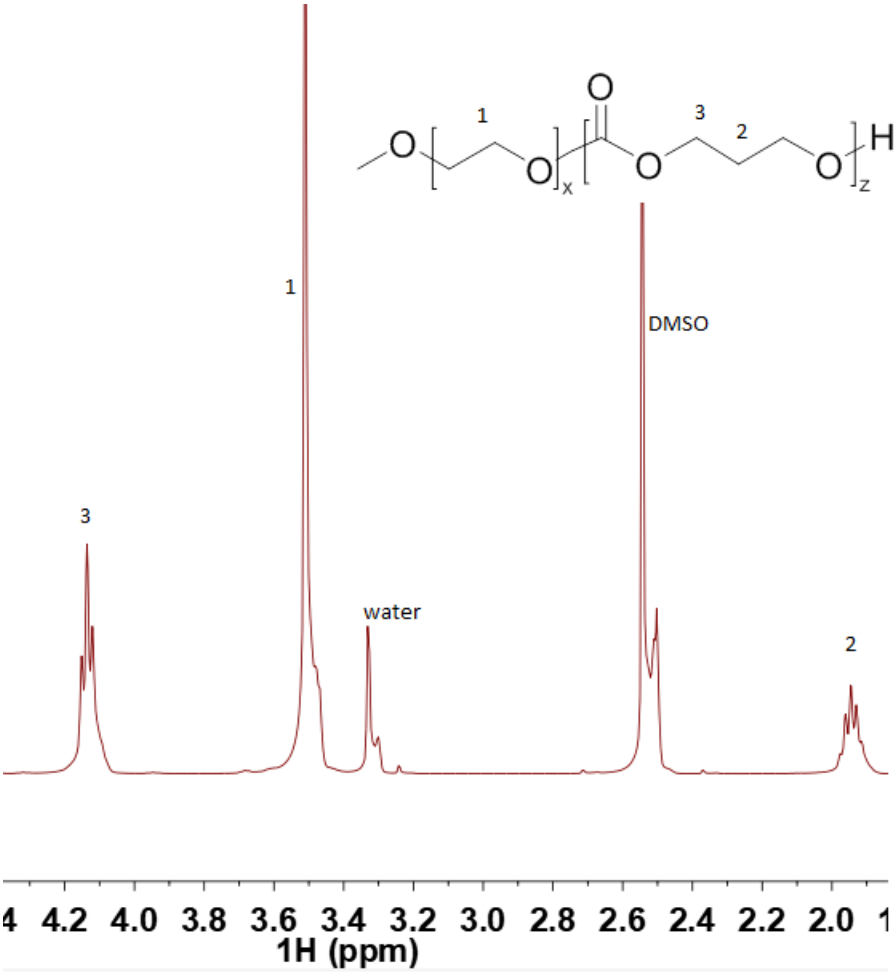

Figure 12: ^{1}H-NMR spectrum of PEG-b-PTMC in d_6-DMSO.

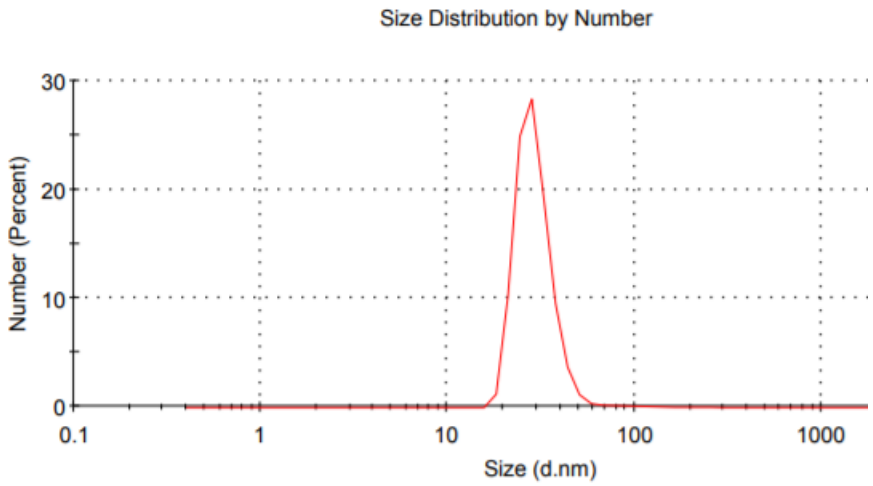

Figure 13: Size distribution by number obtained by DLS for the PEG-b-PTMC loaded micelles.

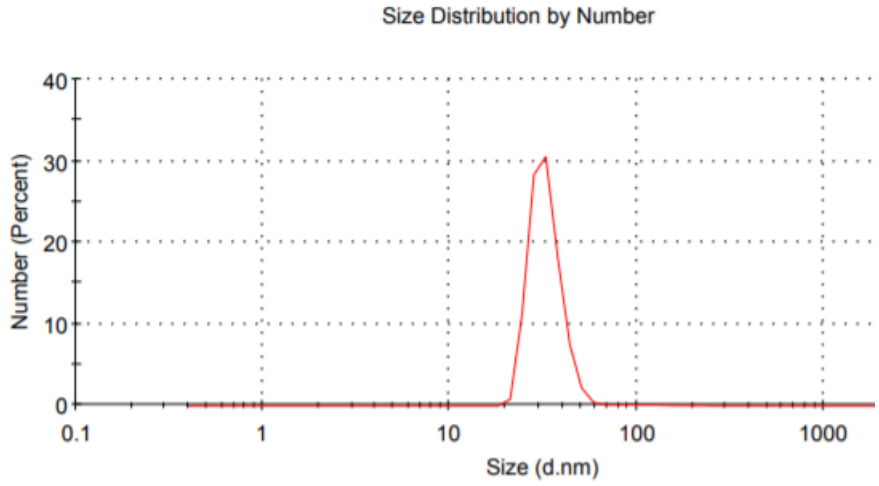

Figure 14: Size distribution by number obtained by DLS for the PEG-b-P(TMC-BTMC) loaded micelles.

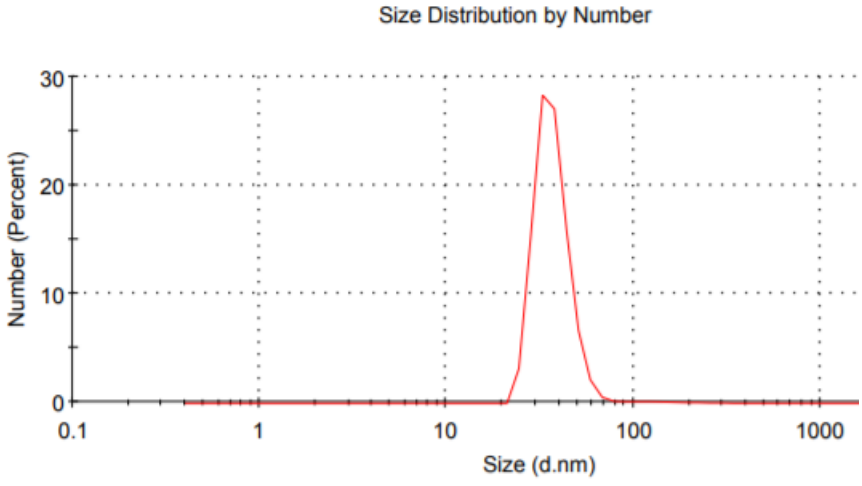

Figure 15: Size distribution by number obtained by DLS for PEG-b-P(TMC-STMC) loaded micelles.

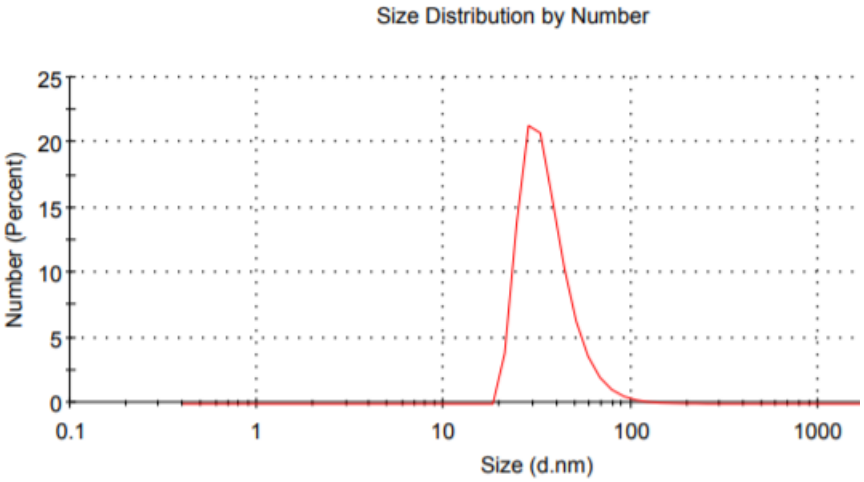

Figure 16: Size distribution by number obtained by DLS for PEG-b-PTMC micelles with no linoleic acid.

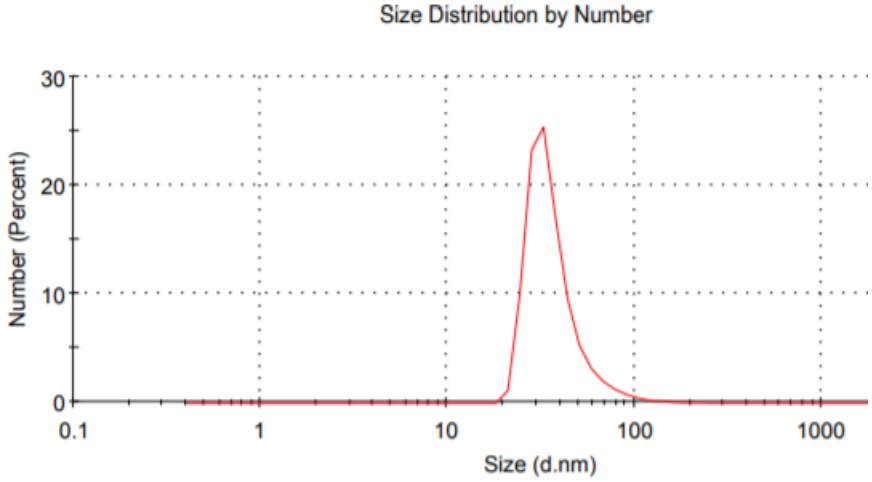

Figure 17: Size distribution by number obtained by DLS for PEG-b-P(TMC-BTMC) micelles with no linoleic acid.

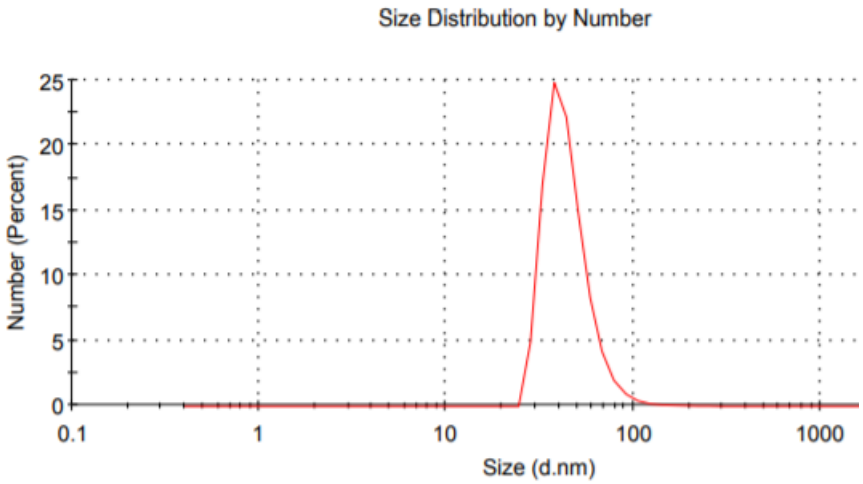

Figure 18: Size distribution by number obtained by DLS for PEG-b-P(TMC-STMC) micelles with no linoleic acid.